Technical Notes

Differential Drag-Based Reference Trajectories for Spacecraft Relative Maneuvering Using Density Forecast

David Pérez* and Riccardo Bevilacqua†
University of Florida, Gainesville, Florida 32611

DOI: 10.2514/1.A33332

Nomenclature

A_{bc}	=	element of matrix A_d to which a_{Dcrit} is the most sensitive
A_d	=	stable linear reference state-space matrix
A_s	=	Schweighart and Sedwick model state-space matrix
a_{Dcrit}	=	magnitude of the differential drag acceleration ensuring stability
a_{Drel}	=	magnitude of the differential aerodynamic drag acceleration
a_{Prelx}, a_{Prely}	=	differential accelerations caused by orbital perturbations excluding drag, along x and y directions of the local vertical/local horizontal frame
C_{DC}, C_{DT}	=	chaser and target spacecraft's drag coefficients
$\boldsymbol{e}$	=	tracking error vector
i_t	=	target's initial orbit inclination
J_2	=	second-order harmonic of Earth gravitational potential field (Earth flattening)
lb, ub	=	lower and upper bounds for the optimization
m_C, m_T	=	chaser and target spacecraft's mass
R_e	=	Earth mean radius
$\boldsymbol{R}_t$	=	position vector of the target in relation to the Earth
S_C, S_T	=	chaser and target spacecraft's crosswind surface area
$\hat{u}$	=	on/off control signal
V	=	Lyapunov function
v_s	=	spacecraft velocity vector magnitude with respect to the Earth's atmosphere
$\boldsymbol{x}_n$	=	state-space vector of the nonlinear system including relative position and velocity between the spacecraft in the local vertical/local horizontal orbital frame
$\boldsymbol{x}_t$	=	reference state-space vector in the local vertical/local horizontal orbital frame
δ_{Aop}	=	modifications made to matrix A_d for the optimized adaptation
μ	=	Earth's gravitational parameter
ρ	=	atmospheric density
ω	=	magnitude of the orbital angular velocity of the target

Received 27 April 2015; revision received 29 September 2015; accepted for publication 20 October 2015; published online 4 January 2016.

*Postdoctoral Researcher, Mechanical and Aerospace Engineering Department, MAE-A Building, P.O. Box 116250; perezd4@ufl.edu. Member AIAA.

†Associate Professor, Mechanical and Aerospace Engineering Department, MAE-A Building, P.O. Box 116250; bevilr@ufl.edu. Senior Member AIAA (Corresponding Author).

I. Introduction

FORMATIONS of small satellites hold the potential for replacing large complex spacecraft, as explained in [1–4]. There are several motivations for developing the technology necessary for spacecraft formations. For example, on-orbit inspections, maintenance missions, and other complex space tasks can be performed using spacecraft formations. A spacecraft formation can survive the failure of one of its satellites without compromising mission objectives, thus providing the benefits of redundancy in its functionality. Additionally, smaller satellites are lighter and can be stacked for launch [5–7], reducing the cost of orbit injection. Consequently, there is a growing interest in the aerospace community on the development of methods for autonomous spacecraft formation flying.

Spacecraft formations require the ability for the spacecraft to control their relative position and velocity. This can be accomplished using thrusters [8], though it may require high operational costs or imposing undesired design constraints. Hence, lower-cost alternatives for maneuvering the spacecraft are of great interest. In their seminal work, Leonard et al. [9] proposed using the drag force that affects the motion of spacecraft at low Earth orbits (LEOs) for controlling their relative motion. Using the differential in the drag accelerations between the spacecraft can allow for propellantless planar relative maneuvering, which can reduce costs for formation-flying missions. Additionally, since no propellant is expelled, sensitive sensors onboard can operate in a cleaner environment. However, using differential drag requires the constraint of operating in LEOs where there is enough atmospheric density for generating differential drag accelerations of sufficient magnitude. Moreover, using differential drag for maneuvering increases the orbital decay of the spacecraft, which can shorten the mission duration.

In this work, it is assumed that the spacecraft have the ability to change their ballistic coefficient. This can be achieved by deploying or retracting a set of drag surfaces, which in principle can be solar panels, as shown in Fig. 1, hence effectively changing the magnitude of the drag force acting on the spacecraft. The local vertical/local horizontal (LVLH) reference frame is used for representing spacecraft relative motion. In this frame, x points from the origin of an inertial frame, located at the center of the Earth, to the target spacecraft; z points in the direction of the orbit angular momentum; and y completes the right-handed frame (see Fig. 1).

Atmospheric differential drag can provide effective control only in the orbital plane (x and y). Hence, the discussion presented in this work will be limited to in-plane motion, assuming the absence of out-of-plane z motion, or that it is controlled by different means. Another assumption is that the attitude of the spacecraft is stabilized by other means than the differential drag. It is worth mentioning that drag can be exploited to control both relative position and orientation of satellites, as demonstrated in [10]. Additionally, we assume that the control is either positive maximum (Fig. 1, case 1), negative maximum (Fig. 1, case 2), or zero (Fig. 1, case 3), as previously done in [11–13], neglecting the time required by the surfaces to be deployed or retracted. This simplification is valid, since the time required to deploy or retract the surfaces (on the order of seconds, or minutes at the most) is negligible with respect to the maneuvers durations (on the order of days).

Maneuvering spacecraft using differential drag is challenging, since the drag force itself is difficult to estimate. For that reason, creating realistic reference trajectories in terms of the control force (drag force) is challenging. This makes maneuvers that require

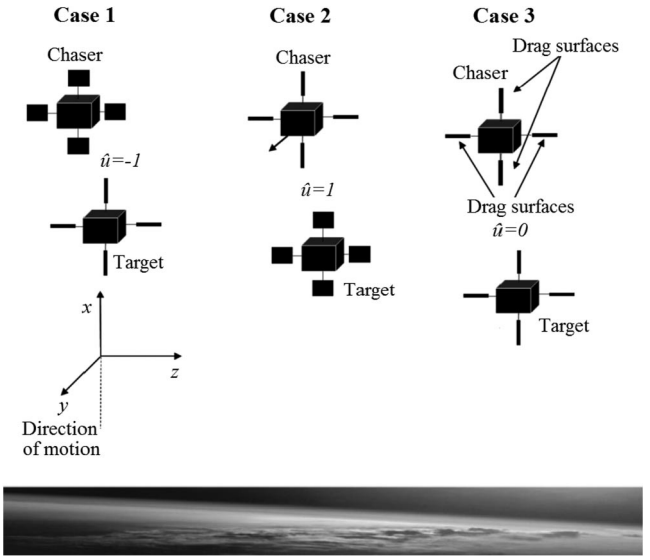

Fig. 1 LVLH frame, chaser and target spacecraft, and drag panels design concept.

following a specific path very difficult to perform. Furthermore, although variable density models are used for simulations, it is usually assumed that the atmospheric density is constant for control and guidance purposes (see [9,14–17]). This is not desirable from the point of view of creating reference trajectories, as this assumption does not account for a realistic behavior of the control force. In [18], Artificial Neural Network (ANN) predictors capable of forecasting the density along the future orbit of a spacecraft were introduced. In the present work, these predictors are used for designing rendezvous reference trajectories created specifically for differential drag-based maneuvering, provided that density estimates or measurements of the present value for the density are available. The advancement on the state of the art in this work is the integration of the neural network predictors with a control method (developed in [19–24]) for generating reference trajectories specially designed for relative maneuvering using differential drag. The resulting reference trajectory provides unprecedented accuracy in terms of the drag force, allowing for better reference tracking.

This Note is organized as follows. Section II presents the basic principles for spacecraft relative maneuvering using differential drag, including the nonlinear and linear relative dynamics equations, and an optimized adaptive Lyapunov controller especially designed for drag relative maneuvering. Section III presents a reference trajectory for a rendezvous maneuver using predicted density, and Systems Tool Kit (STK) simulation of the optimized adaptive Lyapunov controller used for tracking the reference trajectory. Section IV presents the conclusions.

II. Spacecraft Relative Maneuvering Using Differential Drag

A. Nonlinear Relative Dynamics

The following equations represent the relative motion dynamics for a chaser and target spacecraft in the LVLH frame:

$$\dot{\boldsymbol{x}}_n = \begin{bmatrix} \dot{x}_n \\ \dot{y}_n \\ f_x(\boldsymbol{x}_n) \\ f_y(\boldsymbol{x}_n) \end{bmatrix} + \begin{bmatrix} 0 \\ 0 \\ 0 \\ a_{\text{Drel}} \end{bmatrix} = f(\boldsymbol{x}_n) + \begin{bmatrix} 0 \\ 0 \\ 0 \\ a_{\text{Drel}} \end{bmatrix}$$

$$\ddot{x}_n = f_x(\boldsymbol{x}_n) = \mu\left(\frac{1}{R_t 2} - \frac{R_t + x_n}{((R_t + x_n)^2 + y_n 2)^{3/2}}\right) + 2\omega\dot{y}_n + 2\omega^2 x_n + a_{\text{Prelx}}$$

$$\ddot{y}_n = f_y(\boldsymbol{x}_n) + a_{\text{Drel}} = -\mu\left(\frac{y_n}{((R_t + x_n)^2 + y_n 2)^{3/2}}\right) + 2(\omega^2 y_n - \omega\dot{x}_n) + a_{\text{Prely}} + a_{\text{Drel}} \tag{1}$$

B. Linear Relative Dynamics

The relative nonlinear dynamics have no closed-form solution and do not allow for the use of the numerous techniques developed for linear systems. Therefore, the use of linear dynamics is desired for developing reference trajectories. This section shows the Schweighart and Sedwick [25] linear model used for generating the reference trajectory shown in Sec. III. This model assumes that the target's orbit is circular, that the only perturbation acceleration is caused by the J_2 perturbation, and that the separation between spacecraft is small compared to the radii of their orbits. The Schweighart and Sedwick model can be formulated as the following system:

$$\dot{\boldsymbol{x}}_l = \begin{bmatrix} 0 & 0 & 1 & 0 \\ 0 & 0 & 0 & 1 \\ (5c^2 - 2)n^2 & 0 & 0 & 2nc \\ 0 & 0 & -2nc & 0 \end{bmatrix} \boldsymbol{x}_l + \begin{bmatrix} 0 \\ 0 \\ 0 \\ a_{\text{Drel}} \end{bmatrix}$$

$$= A_s \boldsymbol{x}_l + \begin{bmatrix} 0 \\ 0 \\ 0 \\ a_{\text{Drel}} \end{bmatrix}$$

$$c = \sqrt{1 + \frac{3J_2 R_e}{8R_t^2}[1 + 3\cos(2i_t)]}, \qquad n = \frac{\omega}{c} \tag{2}$$

C. Drag Acceleration and Atmospheric Density

A proper understanding of the drag acceleration will allow for precise orbit determination and can be used for creating realistic maneuvers and reference trajectories using drag. The drag acceleration affecting spacecraft at LEO is a function of the atmospheric winds; the spacecraft's velocity relative to the medium; the spacecraft's geometry, attitude, drag coefficient, and mass; and, most important, the atmospheric density. Due to the mutual dependencies of these parameters and the lack of knowledge in their dynamics, modeling the drag force proves to be a difficult problem. This results in large uncertainties regarding the control forces available for maneuvers using drag forces.

The magnitude of the relative acceleration caused by the differential aerodynamic drag for target and chaser is usually expressed as

$$a_{\text{Drel}} = \frac{1}{2}\rho\left(\frac{C_{D_C} S_C}{m_C} - \frac{C_{D_T} S_T}{m_T}\right) v_s^2 \tag{3}$$

where C_D, S, and m are the drag coefficient, the crosswind surface area of the spacecraft, and the mass of the spacecraft, respectively. The subindices C and T refer to the chaser and target spacecraft.

As was shown in [18], out of all the elements in Eq. (3), the density is the one that varies the most. Furthermore, at an altitude of 400 km, density can vary by more than one order of magnitude at a given time [26]. Therefore, the largest errors in the drag acceleration estimation come from density estimation errors. Furthermore, according to [27], the density represents the largest contribution of errors in any orbit determination application. For these reasons, accurate modeling and forecasting of the density is required for generating realistic reference trajectories for maneuvering spacecraft using drag. In contrast, the drag coefficient according to [27] is bounded between two and four; according to [28], it can be modeled accurately using direct Monte Carlo simulations (differences of ~0.1% when compared with closed-form solutions). The velocity of the spacecraft relative to the medium is traditionally defined as the velocity of the spacecraft minus the velocity of the atmosphere. In this case, the greatest source of uncertainty comes from the atmospheric winds; however, their magnitude (on the order of hundreds of meters per second according to [27]) is smaller than the magnitude of the spacecraft speed (on the

order of kilometers per second). Consequently, in this work, the focus is on improving the reference trajectory for drag maneuvering using the neural network forecasted density; nevertheless, future work should address the effects of the errors in atmospheric wind and drag coefficient modeling, as well as how to mitigate them.

Empirical atmospheric models such as NRLMSISE-00 (see [29]) can provide density estimation at the present, provided that the solar and geomagnetic indices are known. Current values for these indices are available online and are updated at their respective latencies (see [30] for one of the databases where these values can be obtained). However, these models also require averaged values of these indices over periods covering both the past and future of the instance at which the density is estimated. To obtain these averaged indices, a forecast of the indices can be used such as the ones provided by the National Oceanic and Atmospheric Administration (see [31]). It should be mentioned that the accuracy of the empirical models will be impacted by the forecasting error. Furthermore, there are models such as the High-Accuracy Satellite Drag Model (HASDM; see [32]) that provide highly accurate density estimations in almost real time. Unfortunately, access to the HASDM is restricted. Finally, the density can also be measured onboard using sensors such as those included in the Winds-Ions-Neutral Composition Suite (see [33]).

D. Lyapunov Controller

In previous work [19], Lyapunov principles were used to design a control law for the drag surfaces that generated the differential drag. The value of the control signal was selected so that the Lyapunov function was positive and its time derivative [both shown in Eq. (4)] was negative, which ensured that the tracking error converged to zero. The Lyapunov controller was used to force the nonlinear model [Eq. (2)] to track the reference trajectory $\boldsymbol{x}_t$:

$$V = \boldsymbol{e}^T P \boldsymbol{e}, \quad \boldsymbol{e} = \boldsymbol{x}_n - \boldsymbol{x}_t, \ \dot{V} = 2\boldsymbol{e}^T P(\boldsymbol{f}(\boldsymbol{x}_n) - \dot{\boldsymbol{x}}_t + \boldsymbol{B} a_{\text{Drel}} \hat{u}) \tag{4}$$

where $\hat{u}$ is the command sent to the surface actuators, the matrix Q is chosen such that a Lyapunov equation is satisfied ($A_d^T P + P A_d = -Q$), and the matrices A_d and $\boldsymbol{B}$ represent stable linear reference dynamics, which were created by using a linear quadratic regulator to stabilize the Schweighart and Sedwick dynamics [25]. The resulting control law presented in [19] can be expressed as

$$\hat{u} = -\text{sign}(\boldsymbol{e}^T P \boldsymbol{B}) \tag{5}$$

The meaning of the resulting value for $\hat{u}$ is explained in Fig. 1. A critical value a_{Dcrit} of differential drag that is needed to maintain stable Lyapunov control was developed in [20,21]. This critical value, for the case in which the nonlinear dynamics are tracking a reference trajectory, is given as

$$a_{\text{Dcrit}} = \frac{\boldsymbol{e}^T P(\dot{\boldsymbol{x}}_t - \boldsymbol{f}(\boldsymbol{x}_n))}{|\boldsymbol{e}^T P \boldsymbol{B}|} \tag{6}$$

The analytical expression for the partial derivative of the critical value with respect to the matrix A_d was developed in [22,23]. The matrix A_d is set by design, so it can be manipulated to reduce the value of the critical value during the maneuver, provided that it remains Hurwitz. The element of matrix A_d, to which a_{Dcrit} is the most sensitive (A_{bc}; the entry with the largest partial derivative) is identified by calculating the partial derivative. Next, MATLAB's fmincon function is used to minimize a_{Dcrit} in terms of A_{bc}. The optimization problem, solved by fmincon, can be formulated as

$$\begin{aligned} &\underset{A_{bc}}{\text{minimize}} \quad a_{\text{Dcrit}}(A_{bc}) \\ &\text{subject to} \quad lb \le A_{bc} \le ub \end{aligned} \tag{7}$$

where lb and ub are the lower and upper bounds for A_{bc}. These bounds were selected to be -10^{-6} and 10^{-6}, which are on the same order of magnitude as the other entries of A_d. The solution of the optimization problem provides the sign and magnitude δ_{Aop} with which A_{bc} is modified. The adaptive variations in A_d can be written as

$$\frac{\Delta A_{ij}}{\Delta t} = \kappa_A \delta_{\text{Aop}}, \quad \kappa_A = \begin{cases} 1 & \text{if } \left|\frac{\partial a_{\text{Dcrit}}}{\partial A_{ij}}\right| > \left|\frac{\partial a_{\text{Dcrit}}}{\partial A_{kl}}\right| \ \text{ for } i,j \neq k,l \\ 0 & \text{else} \end{cases} \tag{8}$$

The adaptation, which consists of calculating the partial derivative, determining A_{bc}, performing the optimization, and applying Eq. (8) to obtain the new A_d, occurs every 10 min. The adapted A_d is used along with Q (which is not adapted) to obtain P and the control signal $\hat{u}$, at each adaptation time (every 10 min). Between adaptations, A_d remains constant. Furthermore, for a bang-off-bang control (i.e., the controls changes instantly and the adaptation is instantaneous), the Δt is essentially zero. By reducing this critical value, the overall robustness of the controller is improved, since the control margin (the difference between the actual value of the differential drag acceleration and the critical value) is increased.

III. Reference Trajectory for a Rendezvous Maneuver

To create the reference trajectory using predicted density, the methodology presented in [18] is exploited. In particular, an STK scenario, in which NRLMSISE-00 is used for modeling the density, was propagated using STK's high-precision orbit propagator (HPOP) for a period of four days before and two days after the maneuver's initial time. The scenario contained the target spacecraft with half of its drag area deployed. The density data along the target's orbit were sampled and imported to MATLAB. The density data from the first two days were used for training and validating a neural network predictor with a prediction window of 30 orbits (about two days). The neural network used had one neuron in the hidden layer and 690 delays (1/4 of the prediction window of 30 orbits). The resulting neural network had a performance of MSE = 1.0497e-04 and $R_p = 0.9997$. These metrics are much better than those observed with the neural network predicting 32 orbits for the CHAMP data presented in [18]. This is explained by the fact that the density estimated by the NRLMSISE-00 has a simpler behavior than the density estimated from the CHAMP's accelerometers used in [18].

The linear model shown in Eq. (2) was regulated using the Lyapunov controller shown in Eq. (5), without adaptation, to create the reference trajectory to achieve a rendezvous. Additionally, a second reference trajectory was generated with a constant value for the density (the density averaged over the training and validating datasets), again by regulating the linear model using the Lyapunov controller. This constant density case serves as a benchmark for the first case, which uses forecasted density. The two reference trajectories in the LVLH frame are shown in Fig. 2.

The orbital elements of the target at the beginning of the maneuver, and other parameters are shown in Table 1. The target and chaser spacecraft are identical. The initial condition for the state vector is shown in Table 2. The orbits of both spacecraft are coplanar; therefore, the position and velocity of the chaser relative to the target on the z direction are zero.

The reference trajectory that used the predicted density had 54 control changes and lasted for 27.3 h, whereas the reference trajectory that used the constant density had 83 control changes and lasted for 20.6 h.

A. Numerical Simulations Results

To observe the advantages of using the reference trajectory with the predicted density, the optimized adaptive controller [Eqs. (5), (7), and (8)] was used for forcing the nonlinear dynamics of the chaser and target spacecraft to track the reference trajectories. The nonlinear dynamics were propagated using HPOP. The simulations were stopped when the target and chaser were within 10 m of each other. Figure 3 shows the trajectories when tracking the reference trajectory obtained with the constant density (left plot) and the reference trajectory obtained with the predicted density from the ANN (right plot), respectively. Figure 4 displays the tracking errors. Finally, Fig. 5 shows the control signals when tracking the reference trajectory obtained with the constant density (top plot) and the reference trajectory obtained with the predicted density from the ANN (bottom plot), respectively.

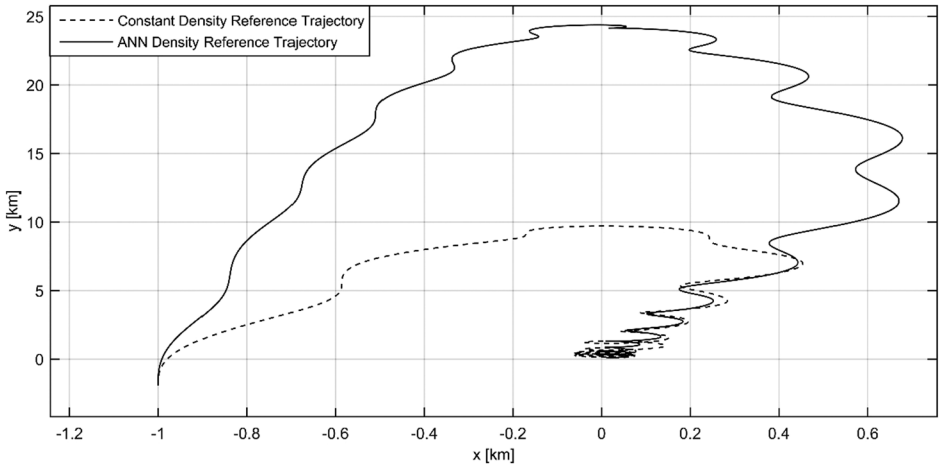

Fig. 2 Reference trajectories in the *x*-*y* plane for a rendezvous maneuver generated with the predicted and constant density.

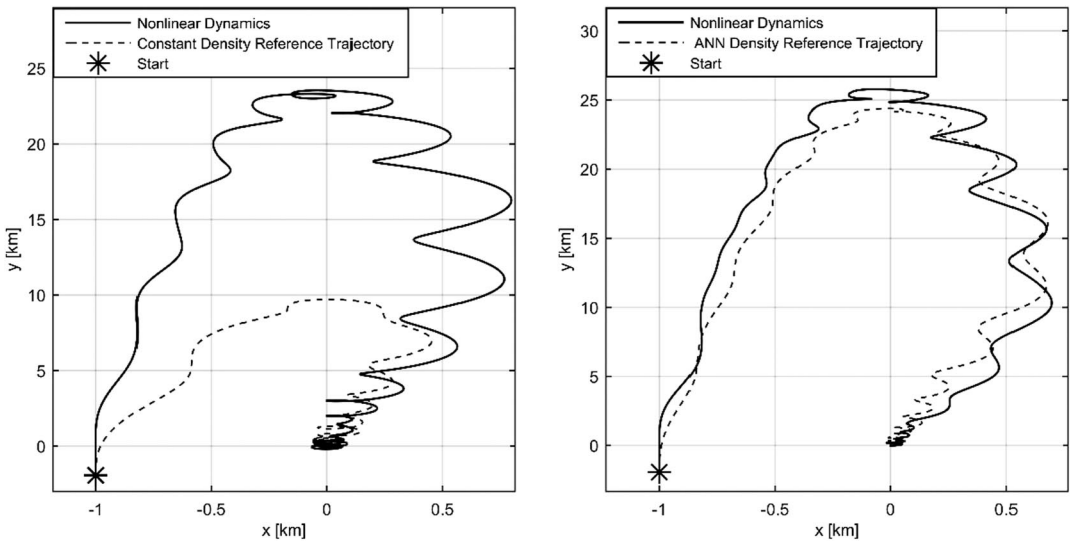

Fig. 3 Rendezvous trajectories in the *x*-*y* plane.

The most prominent features seen in Fig. 4 are the large spikes in the tracking errors for the case in which the system is tracking the reference trajectory generated with the constant density. This indicates how difficult it is for the controller to force the nonlinear dynamics to follow the reference trajectory generated with the constant density. The reason for this is that the reference trajectory with the constant density does not represent the complex behavior of the density; consequently, it is not a suitable trajectory to track with differential drag. In contrast, tracking the reference trajectory generated with the predicted density yields much smaller tracking errors (about one order of magnitude smaller in the y direction and less than half in the x direction). This clearly shows how much easier it is for the system to track the reference trajectory generated with the predicted density over the scenario with the constant density. Realistic reference trajectories will provide a good idea of how the nonlinear system will behave. This allows for performing maneuvers using differential drag in which a path can be followed closely. This is critical for complex maneuvers with more than two spacecraft in which the possibility of spacecraft collisions is a significant issue.

Table 1 Spacecraft parameters

Parameter	Value
Target's inclination, deg	98
Target's semimajor axis, km	6778
Target's right ascension of the ascending node, deg	262
Target's argument of perigee, deg	30
Target's true anomaly, deg	25
Target's eccentricity	0
Target's speed, km/s	7.68
Spacecraft mass m, kg	10
Surface retracted $S_{\min}$, m^2	0.3409
Surface deployed $S_{\max}$, m^2	2.8409
C_D	2.2

B. Performance Assessment and Discussion

Table 3 shows the metrics used to evaluate the performances obtained with the two different reference trajectories: the number of changes in the control (control effort), the time it took for the spacecraft to be within 10 m of their desired final state, the mean values for the critical and actual value of the differential drag acceleration, and the control margin that is the difference between these two values. Table 3 shows that the maneuver that used the reference trajectory created with predicted density reached the desired final point much faster, and with less control effort than the one that used the reference trajectory generated with the constant density.

Table 2 Initial conditions in the LVLH frame

Parameter	Rendezvous
x^n, km	-1
y^n, km	-2
$\dot{x}_n$, km/s	$4.83 \cdot 10^{-07}$
$\dot{y}_n$, km/s	$1.70 \cdot 10^{-04}$

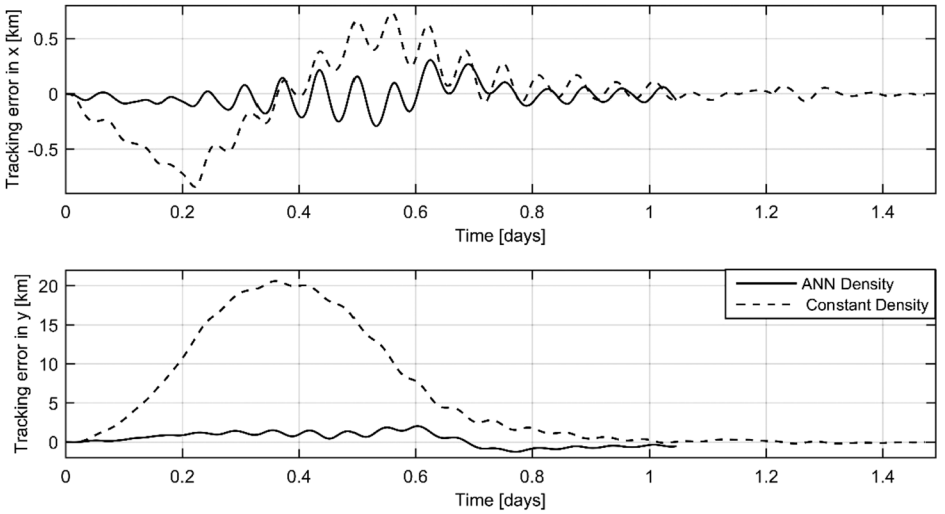

Fig. 4 Tracking error over the entire rendezvous maneuver: (top) *x* error, and (bottom) *y* error.

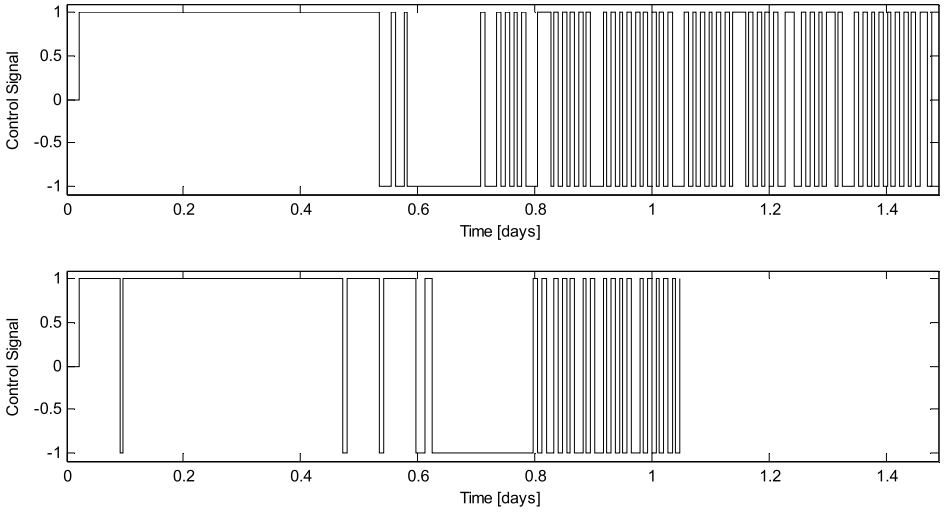

Fig. 5 Rendezvous maneuver control signals.

The availability of the drag predictors opens up many possibilities for creating realistic optimal reference trajectories especially designed for relative maneuvering using differential drag, provided that these maneuvers are short enough that the predictor can accurately forecast the density. The development of these optimal trajectories would be an interesting extension for the research presented here.

It is important to note that the method used for obtaining the predicted density is not realistic from an implementation point of view. This is because the values for the density used as inputs to the neural network predictor and the density used to propagate the maneuver itself were obtained from the same atmospheric model (NRLMSISE-00). This means that the guidance software has perfect measurements of the density along the orbit of the spacecraft, before the maneuver. In a real-world application, the density would be obtained from either an atmospheric density model or from sensors onboard the spacecraft, both of which result in a bias in the estimated/measured density. This would increase the error in the predicted density. The effects of these estimation/measurement errors must be studied. Furthermore, the effect of modeling errors in the drag coefficient and the atmospheric wind on the reference trajectory should be studied.

Table 3 Control performance metrics for the rendezvous maneuver tracking the reference trajectory obtained with the constant density and the predicted density from the ANN

Case	Metric	Rendezvous
Density from NN	Control changes	43
	Time, h	25.0833
	Drag mean critical value, m/s^2	1.05E-04
	Mean actual drag, m/s^2	3.50E-05
	Margin, m/s^2	−7.01E-05
Constant density	Control changes	99
	Time, h	35.35
	Drag mean critical value, m/s^2	6.33E-05
	Mean actual drag, m/s^2	3.53E-05
	Margin, m/s^2	−2.80E-05

IV. Conclusions

The last decades have seen a growing interest in small spacecraft formations and the potential of using natural means to control them without use of propellant. The differential drag idea falls under this category, and it presents challenging problems, especially the need for good models for the atmospheric neutral density. This work presented the utilization of artificial neural networks to predict the future behavior of the density, enabling design of realistic differential drag-based reference trajectories for relative maneuvers. The neural network density predictors are integrated with a controller to create a reference trajectory. The results of the simulations show that a controller is capable of more closely tracking the reference trajectory generated using the predicted density, compared to the commonly used constant density assumption. This indicates that the density predictors can be used for generating realistic reference trajectories for relative differential drag-based maneuvering of spacecraft.

Acknowledgments

The authors wish to acknowledge the Office of Naval Research, Young Investigator Program, for sponsoring this investigation (award no. N00014-15-1-2087). The results presented in this document were included in the doctoral thesis of one of the authors.

References

[1] Kapila, V., Sparks, A. G., Buffington, J. M., and Yan, Q., "Spacecraft Formation Flying: Dynamics and Control," *Journal of Guidance, Control, and Dynamics*, Vol. 23, No. 3, 2000, pp. 561–564. doi:10.2514/2.4567

[2] Sabol, C., Burns, R., and McLaughlin, C. A., "Satellite Formation Flying Design and Evolution," *Journal of Spacecraft and Rockets*, Vol. 38, No. 2, 2001, pp. 270–278. doi:10.2514/2.3681

[3] Scharf, D. P., Hadaegh, F. Y., and Ploen, S. R., "A Survey of Spacecraft Formation Flying Guidance and Control (Part 1): Guidance," *Proceedings of the American Control Conference*, Vol. 2, IEEE Publ., Piscataway, NJ, June 2003, pp. 1733–1739. doi:10.1109/ACC.2003.1239845

[4] Scharf, D. P., Hadaegh, F. Y., and Ploen, S. R., "A Survey of Spacecraft Formation Flying Guidance and Control. Part II: Control," *Proceedings of the American Control Conference*, Vol. 4, IEEE Publ., Piscataway, NJ, June 2004, pp. 2976–2985.

[5] Heidt, H., Puig-Suari, J., Moore, A., Nakasuka, S., and Twiggs, R., "CubeSat: A New Generation of Picosatellite for Education and Industry Low-Cost Space Experimentation," *Proceedings of the 14th Annual AIAA/USU Conference on Small Satellites*, Utah State Univ., Logan, UT, Sept. 2000, pp. 1–19.

[6] Puig-Suari, J., Turner, C., and Twiggs, R., "CubeSat: The Development and Launch Support Infrastructure for Eighteen Different Satellite Customers on One Launch," *Proceedings of the 15th Annual AIAA/USU Conference on Small Satellites*, Utah State Univ., Logan, UT, Aug. 2001, pp. 1–5.

[7] Puig-Suari, J., Turner, C., and Ahlgren, W., "Development of the Standard CubeSat Deployer and a CubeSat Class PicoSatellite," *Proceedings of the Aerospace Conference*, Vol. 1, IEEE Publ., Piscataway, NJ, March 2001, pp. 1347–1353. doi:10.1109/AERO.2001.931726

[8] Burges, J. D., Hall, M. J., and Lightsey, E. G., "Evaluation of a Dual-Fluid Cold-Gas Thruster Concept," *International Journal of Mechanical and Aerospace Engineering*, Vol. 6, No. 8, 2012, pp. 232–237.

[9] Leonard, C. L., Hollister, W. M., and Bergmann, E. V., "Orbital Formationkeeping with Differential Drag," *Journal of Guidance, Control and Dynamics*, Vol. 12, No. 1, 1989, pp. 108–113. doi:10.2514/3.20374

[10] Pastorelli, M., Bevilacqua, R., and Pastorelli, S., "Differential-Drag-Based Attitude and Position Control for Propellant-Less Spacecraft Rendezvous," *Acta Astronautica*, Vol. 114, 2015, pp. 6–21. doi:10.1016/j.actaastro.2015.04.014

[11] Kumar, B., Ng, A., Yoshihara, K., and De Ruiter, A., "Differential Drag as a Means of Spacecraft Formation Control," *Proceedings of the 2007 IEEE Aerospace Conference*, IEEE Publ., Piscataway, NJ, March 2007, pp. 1–9. doi:10.1109/AERO.2007.352790

[12] Kumar, B. S., and Ng, A., "A Bang-Bang Control Approach to Maneuver Spacecraft in a Formation with Differential Drag," *AIAA Guidance, Navigation, Control Conference, and Exhibit*, AIAA Paper 2008-6469, Aug. 2008, pp. 18–21. doi:10.2514/6.2008-6469

[13] Bevilacqua, R., and Romano, M., "Rendezvous Maneuvers of Multiple Spacecraft by Differential Drag under J_2 Perturbation," *Journal of Guidance, Control and Dynamics*, Vol. 31, No. 6, 2008, pp. 1595–1607. doi:10.2514/1.36362

[14] Bevilacqua, R., Hall, J. S., and Romano, M., "Multiple Spacecraft Assembly Maneuvers by Differential Drag and Low Thrust Engines," *Celestial Mechanics and Dynamical Astronomy*, Vol. 106, No. 1, 2010, pp. 69–88. doi:10.1007/s10569-009-9240-3

[15] Harris, M. W., and Açıkmeşe, B., "Minimum Time Rendezvous of Multiple Spacecraft Using Differential Drag," *AIAA Guidance, Navigation, and Control (GNC) Conference*, AIAA Paper 2013-2385, Aug. 2013. doi:10.2514/6.2013-4775

[16] Pérez, D., and Bevilacqua, R., "Feedback Control of Spacecraft Rendezvous Maneuvers Using Differential Drag," *Proceedings of the 4th International Conference on Spacecraft Formation Flying Missions & Technologies*, Interscience, Saint-Hubert, QBC, Canada, May 2011, pp. 1–10.

[17] Bevilacqua, R., "Analytical Guidance Solutions for Spacecraft Re-Phasing Based on Input Shaping," *Journal of Guidance, Control, and Navigation*, Vol. 37, No. 3, 2014, pp. 1042–1047. doi:10.2514/1.G000008

[18] Pérez, D., Wohlberg, B., Lovell, T., Shoemaker, M., and Bevilacqua, R., "Orbit-Centered Atmospheric Density Prediction Using Artificial Neural Networks," *Acta Astronautica*, Vol. 98, May–June 2014, pp. 9–23. doi:10.1016/j.actaastro.2014.01.007.

[19] Pérez, D., and Bevilacqua, R., "Lyapunov-Based Spacecraft Rendezvous Maneuvers Using Differential Drag," *AIAA Guidance, Dynamics, and Control Conference*, AIAA Paper 2011-6630, Aug. 2011, pp. 7231–7253. doi:10.2514/6.2011-6630

[20] Pérez, D., and Bevilacqua, R., "Differential Drag Spacecraft Rendezvous Using an Adaptive Lyapunov Control Strategy," *Proceedings of the 1st International Academy of Astronautics Conference on Dynamics and Control of Space Systems*, Univelt, Porto, Portugal, March 2012, pp. 973–991.

[21] Pérez, D., and Bevilacqua, R., "Differential Drag Spacecraft Rendezvous Using an Adaptive Lyapunov Control Strategy," *Acta Astronautica*, Vol. 83, Feb.–March 2013, pp. 196–207. doi:10.1016/j.actaastro.2012.09.005

[22] Pérez, D., and Bevilacqua, R., "Spacecraft Maneuvering via Atmospheric Differential Drag Using an Adaptive Lyapunov Controller," *Proceedings of the 23rd AAS/AIAA Spaceflight Mechanics Meeting*, Univelt, Escondido, CA, Feb. 2013, pp. 1–20.

[23] Pérez, D., and Bevilacqua, R., "Lyapunov-Based Adaptive Feedback for Spacecraft Planar Relative Maneuvering via Differential Drag," *Journal of Guidance, Control, and Dynamics*, Vol. 37, No. 5, 2014, pp. 1678–1684. doi:10.2514/1.G000191

[24] Pérez, D., "Adaptive Lyapunov Control and Artificial Neural Networks for Spacecraft Relative Maneuvering Using Atmospheric Differential Drag," Ph.D. Dissertation, Mechanical, Aerospace, and Nuclear Engineering Dept., Rensselaer Polytechnic Inst., Troy, NY, 2013.

[25] Schweighart, S. A., and Sedwick, R. J., "High-Fidelity Linearized J_2 Model for Satellite Formation Flight," *Journal of Guidance, Control, and Dynamics*, Vol. 25, No. 6, 2002, pp. 1073–1080. doi:10.2514/2.4986

[26] Doornbos, E., Forster, M., Fritsche, B., van Helleputte, T., van den IJssel, J., Koppenwallner, G., Luhr, H., Rees, D., and Visser, P., "ESTEC Contract 21022/07/NL/HE Air Density Models Derived from Multi-Satellite Drag Observations—Final Report," DEOS/Delft Univ. of Technology Scientific TR 01/2009, Delft, The Netherlands, 2009, pp. 7–39.

[27] Vallado, D. A., and Finkleman, D., "A Critical Assessment of Satellite Drag and Atmospheric Density Modeling," *Acta Astronautica*, Vol. 95, Feb.–March 2014, pp. 141–165. doi:10.1016/j.actaastro.2013.10.005

[28] Mehta, P. M., Walker, A., McLaughlin, C. A., and Koller, J., "Comparing Physical Drag Coefficients Computed Using Different Gas-Surface Interaction Models," *Journal of Spacecraft and Rockets*, Vol. 51, No. 3, 2014, pp. 873–883. doi:10.2514/1.A32566

[29] Picone, J. M., Hedin, A. E., Drob, D. P., and Aikin, A. C., "NRLMSISE-00 Empirical Model of the Atmosphere: Statistical Comparisons and Scientific Issues," *Journal of Geophysical Research*, Vol. 107, No. A12, 2002, pp. SIA 15-1–SIA 15-16. doi:10.1029/2002JA009430

[30] *OMNIWeb* [online database], Goddard Space Flight Center Space Physics Data Facility http://omniweb.gsfc.nasa.gov/ow.html [retrieved 14 July 2015].

[31] *Space Weather Prediction Center* [online database], National Oceanic and Atmospheric Administration, http://www.swpc.noaa.gov/forecasts [retrieved 14 July 2015].

[32] Storz, M. F., Bowman, B. R., Branson, M. J. I., Casali, S. J., and Tobiska, W. K., "High Accuracy Satellite Drag Model (HASDM)," *Advances in Space Research*, Vol. 36, No. 12, 2005, pp. 2497–2505. doi:10.1016/j.asr.2004.02.020

[33] Nicholas, A. C., Herrero, F., Finne, T. T., and Jones, H. H., "The Winds-Ions-Neutral Composition Suite (WINCS)," *Abstract SA11A-1563 Presented at 2010 Fall Meeting*, AGU, San Francisco, CA, Dec. 2010, p. 1563.

D. Geller
Associate Editor